Coding for stable transmission of W-band radio-over-fiber system using direct-beating of two independent lasers

L. G. Yang,[1] J. Y. Sung,[1] C. W. Chow,[1,*] C. H. Yeh,[2] K. T. Cheng,[3] J. W. Shi,[4] and C. L. Pan[3]

[1]*Department of Photonics and Institute of Electro-Optical Engineering, National Chiao Tung University, Hsinchu 30010, Taiwan*
[2]*Department of Photonics, Feng Chia University, Seatwen, Taichung 40724, Taiwan*
[3]*Department of Physics and Institute of Photonics Technologies, National Tsing-Hua University, Hsinchu, Taiwan*
[4]*Department of Electrical Engineering, National Central University, Taoyuan, Taiwan*
**cwchow@faculty.nctu.edu.tw*

Abstract: We demonstrate experimentally Manchester (MC) coding based W-band (75 – 110 GHz) radio-over-fiber (ROF) system to reduce the low-frequency-components (LFCs) signal distortion generated by two independent low-cost lasers using spectral shaping. Hence, a low-cost and higher performance W-band ROF system is achieved. In this system, direct-beating of two independent low-cost CW lasers without frequency tracking circuit (FTC) is used to generate the millimeter-wave. Approaches, such as delayed self-heterodyne interferometer and heterodyne beating are performed to characterize the optical-beating-interference sub-terahertz signal (OBIS). Furthermore, W-band ROF systems using MC coding and NRZ-OOK are compared and discussed.

OCIS codes: (060.2330) Fiber optics communications; (060.4510) Optical communications.

References and links

1. C. W. Chow, F. M. Kuo, J. W. Shi, C. H. Yeh, Y. F. Wu, C. H. Wang, Y. T. Li, and C. L. Pan, "100 GHz ultra-wideband (UWB) fiber-to-the-antenna (FTTA) system for in-building and in-home networks," Opt. Express **18**(2), 473–478 (2010).
2. J. Yu, Z. Jia, L. Yi, Y. Su, G.-K. Chang, and T. Wang, "Optical millimeter-wave generation or up-conversion using external modulators," IEEE Photon. Technol. Lett. **18**(1), 265–267 (2006).
3. N. W. Chen, J.-W. Shi, H.-J. Tsai, J.-M. Wun, F.-M. Kuo, J. Hesler, T. W. Crowe, and J. E. Bowers, "Design and demonstration of ultra-fast W-band photonic transmitter-mixer and detectors for 25 Gbits/sec error-free wireless linking," Opt. Express **20**(19), 21223–21234 (2012).
4. F.-M. Kuo, J.-W. Shi, H.-C. Chiang, H.-P. Chuang, H.-K. Chiou, C.-L. Pan, N.-W. Chen, H.-J. Tsai, and C.-B. Huang, "Spectral power enhancement in a 100 GHz photonic millimeter-wave generator enabled by spectral line-by-line pulse shaping," IEEE Photon. J. **2**(5), 719–727 (2010).
5. G.-R. Lin, Y.-C. Chang, and J.-R. Wu, "Rational harmonic mode-locking of erbium-doped fiber laser at 40 GHz using a loss-modulated Fabry–Pérot laser diode," IEEE Photon. Technol. Lett. **16**(8), 1810–1812 (2004).
6. G.-R. Lin, T.-S. Hwang, Y.-H. Chuang, S. C. Wang, and C.-L. Pan, "Broad-band (>20 GHz) laser-diode-based optoelectronic microwave phase shifter," IEEE Trans. Microw. Theory Tech. **46**(10), 1419–1426 (1998).
7. Y.-C. Chi, P.-C. Peng, and G.-R. Lin, "Clock-free RZ-BPSK data generation using self-starting optoelectronic oscillator," J. Lightwave Technol. **29**(11), 1702–1706 (2011).
8. R. W. P. Drever, J. L. Hall, F. V. Kowalsk, G. M. Ford, A. J. Munley, and H. Ward, "Laser phase and frequency stabilization using an optical resonator," Appl. Phys. B **31**(2), 97–105 (1983).
9. B. Dahmani, L. Hollberg, and R. Drullinger, "Frequency stabilization of semiconductor lasers by resonant optical feedback," Opt. Lett. **12**(11), 876–878 (1987).
10. S. L. Woodward, J. W. Stayt, D. M. Romero, J. M. Freund, and G. J. Przybylek, "A study of optical beat interference between Fabry–Perot lasers," IEEE Photon. Technol. Lett. **10**(5), 731–733 (1998).
11. C.-H. Yeh, C.-W. Chow, and C.-L. Pan, "Utilizing erbium fiber ring scheme and Fabry-Perot laser diode for stable and wavelength-tunable laser in single-longitudinal-mode *output*," Laser Phys. Lett. **8**(2), 130–133 (2011).
12. L. A. Johansson and A. J. Seeds, "Millimeter-wave modulated optical signal generation with high spectral purity and wide-locking bandwidth using a fiber-integrated optical injection phase-lock loop," IEEE Photon. J. **12**(6), 690–692 (2000).

#212634 - $15.00 USD Received 22 May 2014; revised 5 Jul 2014; accepted 13 Jul 2014; published 16 Oct 2014

13. T. Nagatsuma, S. Horiguchi, Y. Minamikata, Y. Yoshimizu, S. Hisatake, S. Kuwano, N. Yoshimoto, J. Terada, and H. Takahashi, "Terahertz wireless communications based on photonics technologies," Opt. Express **21**(20), 23736–23747 (2013).
14. Y. Nakasha, M. Sato, T. Tajima, Y. Kawano, T. Suzuki, T. Takahashi, K. Makiyama, T. Ohki, and N. Hara, "W-band transmitter and receiver modules for 10-Gb/s impulse radio," Proc. Microwave Sym. Digest. 553-559 (2009).
15. L. G. Yang, S. S. Jyu, C. W. Chow, C.-H. Yeh, C.-Y. Wong, H.-K. Tsang, and Y. Lai, "A 110 GHz passive mode-locked fiber laser based on a nonlinear silicon-micro-ring-resonator," Laser Phys. Lett. **11**(6), 065101 (2014).
16. J.-W. Shi, F.-M. Kuo, C.-J. Wu, C. L. Chang, C.-Y. Liu, C. Y. Chen, and J.-I. Chyi, "Extremely high saturation current-bandwidth product performance of a near-ballistic uni-traveling-carrier photodiode with a flip-chip bonding structure," IEEE J. Quantum Electron. **46**(1), 80–86 (2010).
17. C. W. Chow, C. H. Yeh, Y. F. Wu, H. Y. Chen, Y. H. Lin, J. Y. Sung, Y. Liu, and C.-L. Pan, "13 Gbit/s WDM-OFDM PON using RSOA-based colourless ONU with seeding light source in local exchange," Electron. Lett. **47**(22), 1235–1236 (2011).

1. Introduction

Millimeter-wave (mm-wave) communications at W-band (75 GHz – 110 GHz) using radio-over-fiber (ROF) technology have attracted attenuations recently [1–4]. For the ROF systems, an optical comb [1, 4] is usually required to produce optical signal for launching into a high speed photodiode (PD) to generate mm-wave signals, in which the wavelength separation between the optical comb lines is equal to the frequency of the mm-wave carrier produced. The optical comb can be generated using a mode-locked pulse laser [1, 5], electro-optical schemes [2, 6, 7], or the direct-beating between two independent continuous-wave (CW) lasers [3]. Among these methods, the direct-beating between two lasers is attractive since the frequency separation of the optical comb lines is not limited by the electrical source. Hence sub-terahertz or terahertz signals can be easily generated and the expensive mode-locked pulse laser is not required. Expensive CW laser source uses external feedback loop (FL), such as frequency tracking circuit (FTC) [8, 9] to maintain the output wavelength stability. For the cost sensitive customer end, low-cost CW laser sources without FTC, such as Fabry-Perot laser diode (FP-LD) [10, 11] are used. However, when using two low-cost CW lasers as local-carrier source in the direct-beating approach, this introduces signal instability in the optical-beating-interference sub-terahertz signal (OBIS) produced by the PD. The signal instability in the OBIS is mainly caused the differences in polarizations and cavity lengths between the two independent CW lasers. The accumulated beating noises, named optical-beating-interference noises (OBIN) are measured. The dominant OBIN is the low-frequency-components (LFCs) beating interference, which are at 10-240 MHz. Such LFCs make a low-frequency modulation to the intermediate frequency (IF) data and reduce the signal-to-noise ratio (SNR).

In this work, we demonstrate experimentally Manchester (MC) coding based W-band ROF system to reduce the LFCs signal distortion by using spectral shaping. Hence, a low-cost and higher performance W-band ROF system is achieved. The error-free transmission (bit-error rate (BER)<10^{-12}) using MC coding is achieved at photocurrent of 5.5 mA and at DC external bias of 1.8 V. It requires 1.6 mA less photocurrent when compared with using non-return-to-zero on-off-keying (NRZ-OOK) signal. The improvement of PD sensitivity is due to the use of MC coding, which exhibits higher tolerance to low-frequency noises, As a result, for the same BER performance, less optical signal power is needed in the MC coding signal than that in NRZ-OOK signal. In this system, direct-beating of two independent low-cost CW lasers without FTC serve as the optical local-carrier (O-LO) to generate the mm-wave. Approaches, such as delayed self-heterodyne interferometer and heterodyne beating are performed to characterize the OBIS. Furthermore, W-band ROF systems using MC coding and NRZ-OOK are compared and discussed.

2. OBIS, OBIN, and LFCs of two independent low-cost CW lasers

At transmitter (Tx) of our ROF system, an data signal is frequency up-converted by O-LO, which is produced by two independently commercial DFB lasers. Although in the experiment, the wavelength separation of the two lasers are 0.8 nm (~100 GHz), in order to fit the measuring bandwidth of the electrical spectrum analyzer (ESA, Agilent E4440A), the

#212634 - $15.00 USD Received 22 May 2014; revised 5 Jul 2014; accepted 13 Jul 2014; published 16 Oct 2014

wavelength separation are at 0.08 nm. Hence, the direct-beating by the two lasers (i.e. the OBIS) corresponds to a 10 GHz tone on electrical spectrum. The setup is shown in Fig. 1(a). It consists of the two CW lasers, a 50:50 optical couplers (CP), two polarization controllers (PCs), a 10 GHz photodiode (PD, Multiplex Inc. MTRX192L). The frequency instability of the 10 GHz tone is shown in Fig. 1(b). The different colors represent the same OBIS which are tracked at different time. The fluctuation over time is within in a range of 240 MHz. It is worth to mention that no FTC is used in our lasers. In the literatures, a stable beating signal can be achieved by optical phase-locked loop [12] or FTC in tunable laser source [13].

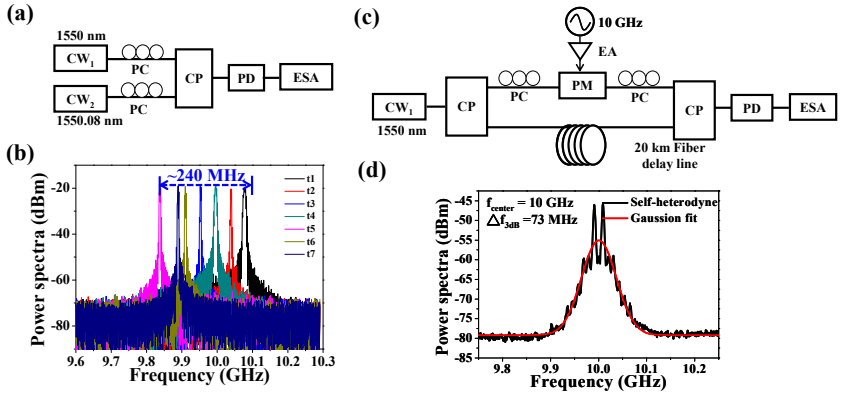

Fig. 1. (a) Experiment of beating by the two lasers. CP: optical coupler, PC: polarization controllers, PD: photodiode, ESA: electrical spectrum analyzer. (b) Measured frequency instabilities. (c) Experiment of delayed self-heterodyne interferometer. (d) Measured linewidth of the CW laser.

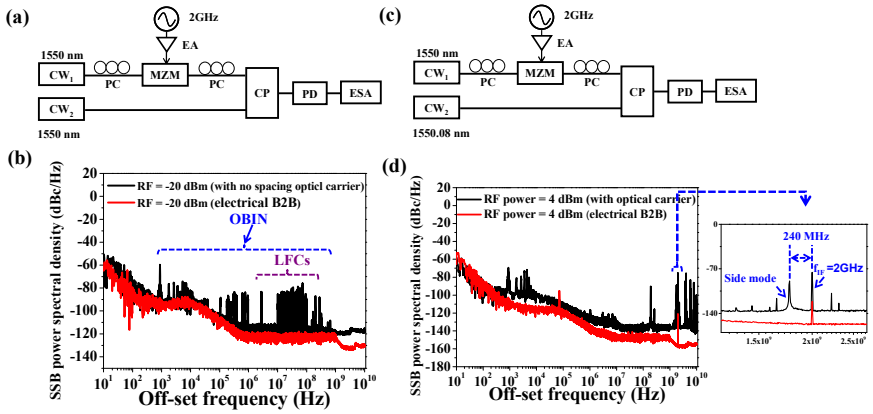

Fig. 2. (a) Experiment of a heterodyne beating of two individual lasers with same wavelength. (b) Measured SSB PSD at carrier frequency of 2 GHz. (c) Experiment of a heterodyne beating of two individual lasers with wavelength separation of 0.08 nm. (b) Measured SSB PSD at carrier frequency of 10 GHz (0.08 nm).

At receiver (Rx) of our ROF system, the OBIS is detected and down-converted by envelope detection. The envelope-detection system can be simpler and less expensive than the coherent-detection system, and no high-speed electrical local oscillators and mixers are needed. The envelope-detection is considered as one of the promising candidates for mm-wave systems [13, 14]. The accumulated beating noises, named OBIN introduce low-frequency modulation to the IF data and reduce the ROF performance. The instability of the two CWs is carried out in following. First, to characterize the dependence of longitudinal modes on polarization state of single CW laser, a delayed self-heterodyne interferometer method was utilized [15]. The setup is shown in Fig. 1(c). It consists of a CW laser, two 50:50 CPs, two PCs, an electrical amplifier (EA), a 10 GHz phase modulator (PM, EOSPACE LN53S-FC), a 10 GHz PD, and an ESA. The CW laser with optical power of 6 dBm is

#212634 - $15.00 USD Received 22 May 2014; revised 5 Jul 2014; accepted 13 Jul 2014; published 16 Oct 2014

launched to a CP and split into two paths. One path is modulated by a 10 GHz sinusoidal signal via a PM and the other path is delayed by a 20 km standard single-mode fiber (SSMF). The delayed heterodyne detection with a 20 km delay length can avoid unwanted beating signals. Finally, OBIS of self-heterodyne is measured by the ESA. The measurement resolution of the method is given by $Res = c/n_dL_d$, where Res is the resolution of measurement, c is the speed of light and n_d and L_d are the refractive index and the length of the fiber delay line, respectively. The presented resolution is about 10 kHz. By Gaussian fitting the measurement results, the 3-dB linewidth of the CW laser was determined to be 73 MHz, as shown in Fig. 1(d).

To further evaluate the effects on OBIN, including unequal polarization state and cavity length of the two independent lasers, a heterodyne beating with a sinusoidal signal is performed for single-sideband (SSB) power spectral density (PSD) measurement, as shown in Fig. 2(a). This measurement is similar to that shown in Fig. 1(c), instead of using a single laser, the two lasers are set at the same wavelength of 1550 nm. The Mach-Zehnder modulator (MZM) is driven by a 2 GHz electrical sinusoidal signal. Figure 2(b) shows the measured SSB PSD, with the carrier frequency at 2 GHz. We can observe all the OBIN, and the dominant LFCs are from 10 MHz to 240 MHz. Then, the wavelength separation of two independent CW lasers is adjusted to 0.08 nm (10 GHz) as shown in Fig. 2(c), and we now measure the SSB PSD at the carrier frequency of 10 GHz (corresponds to the 0.08 nm wavelength separation of the two lasers). By zooming the 2 GHz tone (f_{IF} produced by the modulation via the MZM) of the SSB PSD shown in Fig. 2(d), we can observe the 240 MHz modulation LFCs signal.

3. W-band ROF experiment and results

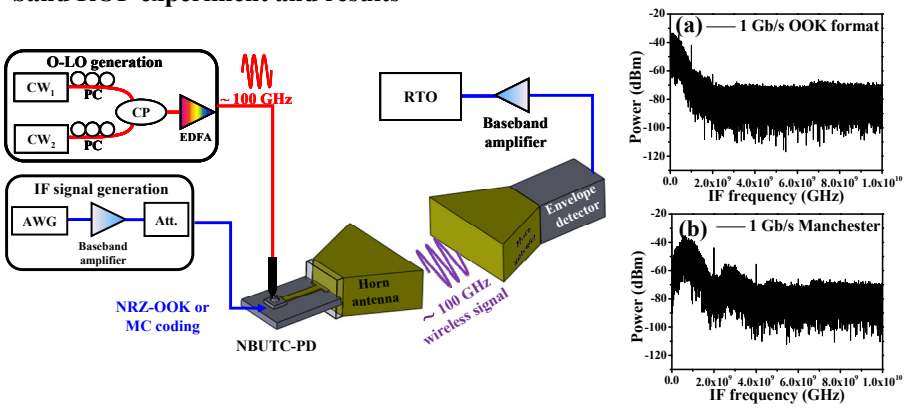

Fig. 3. Experiment of the W-band ROF system. AWG: arbitrary waveform generator, RTO: real-time oscilloscope. Insets: measured power spectra of (a) 1 Gb/s NRZ-OOK coding (b) 1Gb/s MC coding.

Figure 3 shows the experimental setup of the W-band ROF system. The Tx includes the O-LO, an IF generation part and a NBUTC-PD. The wavelength separation between the lasers is 0.8 nm (i.e. 100 GHz). Then the optical signals are combined via a 50:50 CP and then amplified by an erbium doped fiber amplifier (EDFA) before launching into the NBUTC-PD. The NRZ-OOK and the MC coded electrical data are generated by an arbitrary waveform generator (AWG, Tektronix AWG7083C) with sampling rate of 8 GSample/s and bandwidth of 3 GHz. The generated electrical data is amplified and then applied to the NBUTC-PD at the IF port via a bias-tee and an RF probe. DC bias of 1.8 V is used for both NRZ-OOK and MC coding experiments. The function of the NBUTC-PD is a RF mixer for frequency up-converting the IF data to the W-band mm-wave signal, which is then transmitted wirelessly by a W-band horn antenna (Quinstar, QWH-WPRR00). At the Rx, the W-band wireless signal is received by another W-band horn antenna and amplified by a low-noise amplifier (Millitech, LNA-10-02150). The signal is then envelope-detected by an envelope detector

#212634 - $15.00 USD Received 22 May 2014; revised 5 Jul 2014; accepted 13 Jul 2014; published 16 Oct 2014

(Virginia Diodes). The down-converted signal is measured by a real-time oscilloscope (RTO) (Tektronix, DPO7354C) for signal analysis. Insets (a) and (b) of Fig. 3 show the measured power spectra of the two signals. It is observed that most energy of the NRZ-OOK signal is below 1 GHz, while the MC-coded signal is located around the center frequency of 1 GHz.

Our NBUTC-PD [16] has an active area of 100 μm^2. It is flip-chip mounted on a 100μm-thick aluminum nitride (AlN) substrate for good thermal conductivity. Molecular beam epitaxy (MBE) is used to grow the NBUTC-PD on Indium Phosphide (InP). On the AlN substrate, there are also a co-planar waveguide, an intermediate-frequency (IF) input port, a W-band RF choke and a planar quasi-Yagi radiator. The quasi-Yagi radiator is designed so that it can be directly fed into a WR-10 waveguide W-band horn antenna.

The MC encoding and decoding schemes are briefly described here. Figures 4(a) and 4(b) illustrate the schematic bit-patterns of "1011" for the NRZ-OOK and the MC coded signal. As shown in Fig. 4(b), the signal transition from low to high represents logic "1", while the signal transition from high to low represents logic "0". At the Rx, the received MC signal is power divided into two parts. One part is half-bit delayed, as shown in Fig. 4(c). Finally, the received MC signal subtracts its half-bit delayed signal. After this delay-and-subtraction decoding process, the MC signal can be decoded as shown in Fig. 4(d). It can be seen that the original bit-pattern of "1011" can be decoded successfully.

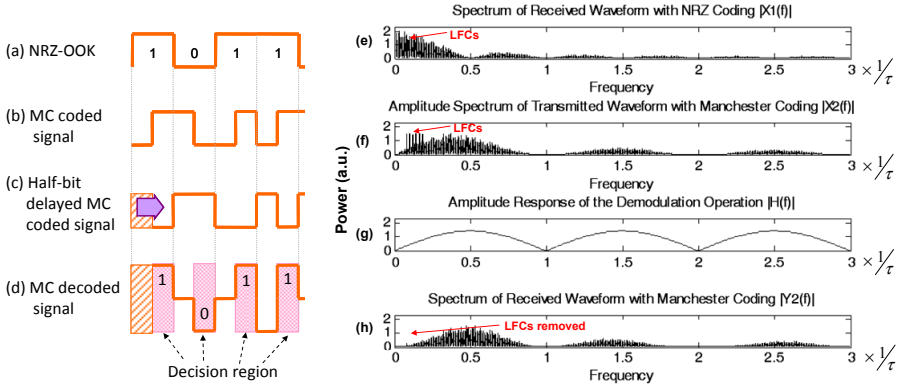

Fig. 4. Schematic bit-patterns of (a) NRZ-OOK, (b) MC signal, (c) half-bit delayed MC signal, and (d) decoded Manchester signal. Simulated power spectra of the (e) received NRZ-OOK signal, (f) received MC coded signal, (g) transfer function of decoding process and (h) decoded MC coded signal.

Then, we analyze the delay-and-subtraction decoding property of the MC coding. It will be shown that this feature makes possible the removal of the LFCs. Since the LFCs cannot be easily extracted from insets (a) and (b) of Fig. 3 directly, a numerical analysis to illustrate the delay-and-subtraction decoding property of MC coding is performed. The MC decoding process can be represented by a transfer function in Eq. (1),

$$h(t) = \delta(t) - \delta(t-\tau) \tag{1}$$

where τ is the half-bit delay time in the decoding process. *H(f)* is the Fourier transform of *h(t)*, can then be expressed in Eq. (2),

$$H(f) = 1 - \exp^{-j2\pi f\tau} \tag{2}$$

The power of the transfer function is then expressed in Eq. (3),

$$\begin{aligned} \left|H(f)\right| &= \left|1-\exp^{-j2\pi f\tau}\right| = \left|\left(1-\cos\left(2\pi f\tau\right)\right) - j\sin\left(2\pi f\tau\right)\right|^2 \\ &= \left(\left(1-\cos\left(2\pi f\tau\right)\right)^2 + \sin^2\left(2\pi f\tau\right)\right)^{\frac{1}{2}} = \left(2\left(1-\cos\left(2\pi f\tau\right)\right)\right)^{\frac{1}{2}} \end{aligned} \tag{3}$$

The transfer function in Eq. (3) does not have a DC (f = 0) component, while its value is a maximum at f = 1/2τ. The simulated power spectra of the NRZ-OOK and MC coding signals, $X_1(f)$ and $X_2(f)$, are shown in Figs. 4(e) and 4(f), respectively. LFCs are added at frequencies from 0.1/τ to 0.2/τ. As the LFCs have high spectral overlapping with the NRZ-OOK signal, it

#212634 - $15.00 USD Received 22 May 2014; revised 5 Jul 2014; accepted 13 Jul 2014; published 16 Oct 2014

has poor signal performance. On the other hand, the received MC coded signal goes through the delay-and-subtraction decoding process, which is equivalent to passing through a periodic band-pass filter shown in Fig. 4(g), which can be described by Eq. (4),

$$Y_2(f) = X_2(f)H(f) \tag{4}$$

As a result, the LFCs in the MC-coded signal can be effectively filtered and removed as presented in the decoded MC coding signal shown in Fig. 4(h). The LFC noise removal is due to the delay-and-subtraction process. When the LFC is at around f = 0, the response of Eq. (3) is zero (this is the stop-band of LFC), and the noise can be removed effectively. When the LFC is at f = 1/2τ (500 MHz in this case), the response of Eq. (3) reaches a maximum value (this is the pass-band for LFC). This means the MC signal has signal improvement when the LFC is at or near the stop-band of Eq. (3), and the signal improvement decreases when the LFC is at or near the pass-band of Eq. (3).

Figure 5(a) shows the measured BER. The MC signal shows a significant transmission enhancement owing to the differential decoding nature discussed above. At BER < 10^{-12}, the photocurrent of 5.5 mA and 7.1 mA respectively, are needed for the MC-coded and NRZ-OOK signals. Compared with the results of using NRZ-OOK under the same DC bias of 1.8 V, 1.6 mA less photocurrent is required in the NBUTC-PD by using the MC coding. At low photocurrent (< 4.5 mA), the BER performance is similar for the MC and NRZ-OOK signals. At higher photocurrent (> 4.5 mA), the NRZ-OOK performs poorer. It is suggested that the influence of LFCs producing the SNR degradation, as shown in measured SNR spectrum of Fig. 5(b). The SNR measurement is based on typical orthogonal frequency division multiplexing (OFDM) signal measurement [17]. The OFDM generation includes serial-to-parallel conversion, quadrature amplitude modulation (QAM) symbol encoding, and inverse fast Fourier transform (IFFT). The OFDM demodulation process includes off-line synchronization, FFT, one-tap equalization, and QAM symbol decoding. Finally, the SNR is measured based on the error vector magnitude (EVM). The OFDM signal produced by the AWG is applied to modulate the NBTUC-PD via a RF probe. A degraded SNR is observed at 240 MHz shown in Fig. 5(b).

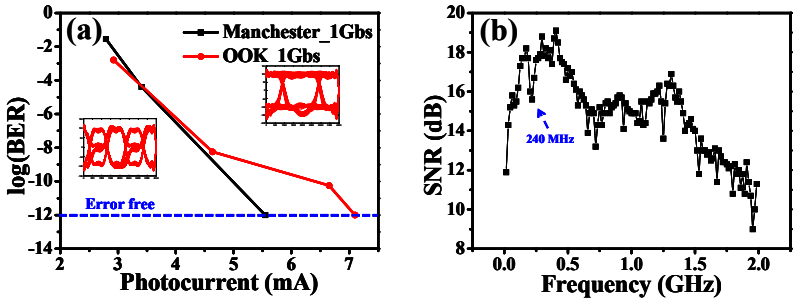

Fig. 5. (a) Measured BER of 1 Gb/s W-band ROF with NRZ-OOK and MC coding, and the corresponding eye-diagrams. (b) SNR performance of the received signal in baseband range from DC to 2 GHz.

4. Conclusion

We experimentally demonstrated MC coding based W-band ROF system to reduce the LFCs signal distortion generated by two independent low-cost lasers by using spectral shaping. Hence, a low-cost and higher performance W-band ROF system was achieved. Approaches, such as delayed self-heterodyne interferometer and heterodyne beating were performed to characterize the OBIS. W-band ROF systems using MC coding and NRZ-OOK were compared and discussed.

Acknowledgments

This work was financially supported by the National Science Council Taiwan, R.O.C., under Contract NSC-101-2628-E-009-007-MY3, NSC-101-2221-E-007-103-MY3, 103-2221-E-009-030-MY3 and Ministry of Education.

#212634 - $15.00 USD Received 22 May 2014; revised 5 Jul 2014; accepted 13 Jul 2014; published 16 Oct 2014